RESEARCH PAPER

Neurite orientation and dispersion density imaging (NODDI) detects cortical and corticospinal tract degeneration in ALS

Rebecca J Broad,[1,2] Matt C Gabel,[1] Nicholas G Dowell,[1] David J Schwartzman,[3] Anil K Seth,[3] Hui Zhang,[4] Daniel C Alexander,[4] Mara Cercignani,[1,5] P Nigel Leigh[1,2]

[1]Department of Neuroscience, Trafford Centre for Biomedical Research, Brighton and Sussex Medical School, Brighton, UK
[2]Brighton and Sussex University Hospitals NHS Trust, Princess Royal Hospital, Haywards Heath, UK
[3]Sackler Centre Consciousness Science, University of Sussex, Brighton, UK
[4]Centre for Medical Image Computing and Department of Computer Science, University College London, London, UK
[5]Neuroimaging Laboratory, Santa Lucia Foundation, Rome, Italy

Correspondence to
Dr Rebecca J Broad, Trafford Centre for Medical Research, Brighton and Sussex Medical School, University of Sussex, Brighton BN1 9RY, UK; r.broad@bsms.ac.uk

ABSTRACT

Background Corticospinal tract (CST) degeneration and cortical atrophy are consistent features of amyotrophic lateral sclerosis (ALS). We hypothesised that neurite orientation dispersion and density imaging (NODDI), a multicompartment model of diffusion MRI, would reveal microstructural changes associated with ALS within the CST and precentral gyrus (PCG) 'in vivo'.

Methods 23 participants with sporadic ALS and 23 healthy controls underwent diffusion MRI. Neurite density index (NDI), orientation dispersion index (ODI) and free water fraction (isotropic compartment (ISO)) were derived. Whole brain voxel-wise analysis was performed to assess for group differences. Standard diffusion tensor imaging (DTI) parameters were computed for comparison. Subgroup analysis was performed to investigate for NODDI parameter differences relating to bulbar involvement. Correlation of NODDI parameters with clinical variables were also explored. The results were accepted as significant where p<0.05 after family-wise error correction at the cluster level, clusters formed with p<0.001.

Results In the ALS group NDI was reduced in the extensive regions of the CST, the corpus callosum and the right PCG. ODI was reduced in the right anterior internal capsule and the right PCG. Significant differences in NDI were detected between subgroups stratified according to the presence or absence of bulbar involvement. ODI and ISO correlated with disease duration.

Conclusions NODDI demonstrates that axonal loss within the CST is a core feature of degeneration in ALS. This is the main factor contributing to the altered diffusivity profile detected using DTI. NODDI also identified dendritic alterations within the PCG, suggesting microstructural cortical dendritic changes occur together with CST axonal damage.

INTRODUCTION

In amyotrophic lateral sclerosis (ALS) degeneration of the corticospinal system, cranial and spinal anterior horn motor neurons is a consistent clinicopathological feature. However, the mechanisms underlying degeneration are not well understood.[1] It is unclear whether degeneration of corticospinal neurons represents a 'dying back' or 'dying forward' process,[2] or whether these categories proposed from histological (ie, end stage) analyses are relevant to the dynamics of cell damage and death in vivo. Understanding these processes is particularly relevant in the context of disease heterogeneity, since there may be common pathways linking the many genetic factors that contribute to pathogenesis.

In this context MRI has provided important insights into the localisation and extent, but not the fine detail, of cellular pathology in ALS. Arguably the most promising application has been diffusion tensor imaging (DTI), a quantitative MRI technique able to indirectly detect microstructural abnormalities due to its sensitivity to water molecule displacement within the tissue.[3 4]

However, DTI has limitations. First, changes to the DTI-derived indices of fractional anisotropy (FA) and mean diffusivity (MD) are non-specific.[5] Second, their interpretation in areas of complex axonal or dendritic architecture is not straightforward.[6 7] Although indices such as the mode of anisotropy can provide some useful information in regions of crossing or fanning,[8] a quantification of neurite density in such areas is challenging with DTI.

Recent developments in diffusion MRI have addressed some of the limitations of standard DTI and advanced capacity to characterise tissue microstructure. Neurite morphology evaluated by diffusion MRI is correlated with histological analyses of neuropil in postmortem brain tissue[9] and with the orientation of neurites in Golgi-impregnated brain tissue in vivo.[10] Neurite orientation dispersion and density imaging (NODDI) provides a simplified yet sophisticated model of diffusion MRI, which separates the signal arising from three different tissue compartments: intraneurite water, extraneurite water and cerebrospinal fluid (CSF).[11 12] This model, recently validated with histological analyses in multiple sclerosis spinal cord,[13] facilitates the analysis of neurite morphology and focuses on quantifying the altered architecture of these multifaceted structures. NODDI estimates the density and fanning of neurites, as well as the partial volume contamination from CSF, using standard MRI scanners within a clinically feasible time frame.

NODDI has been employed in a range of imaging studies, investigating the normal changes observed with ageing,[14] as well as alterations associated with neurodegenerative diseases,[15 16] white matter (WM) reorganisation following stroke[17] and assessment of focal cortical dysplasia.[18] NODDI has also been used to assess WM abnormalities in first-episode psychosis.[19]

We used NODDI to analyse the mechanisms underlying the neurodegenerative changes in ALS.[20 21] Our principal aim was to test the hypothesis that cortical pathology, such as loss or altered complexity of dendrites in the neuropil of the precentral gyrus (PCG), is occurring in ALS. We hypothesised that NODDI would detect reduced neurite density and orientation dispersion, accompanied by an increase in free water compartment. An additional aim was to clarify the microstructural changes within the WM, where we hypothesised that axonal degeneration within the corticospinal tract (CST) would be detected as a loss of neurite density using NODDI.

We used NODDI in parallel with DTI to test the hypothesis that, by removing the confounding effect of orientation dispersion, NODDI would detect more axonal damage within the WM tracts than conventional DTI.

NODDI parameters were used to assess whether a combination of bulbar and limb involvement clinically would reveal differences when compared with limb-confined disease, to test the hypothesis that more widespread clinical involvement would relate to more extensive microstructural damage. Finally correlation of the NODDI parameters with clinical measures of ALS severity was explored with the anticipation that as clinical measures of ALS severity reflect the underlying pathological processes, there may be correlation between these and the NODDI parameters.

This cross-sectional study using NODDI provides the first microstructural analysis of altered density and complexity of neurites in ALS. Analysing these characteristics and how they relate to the disease process 'in vivo' provides an exciting opportunity to advance the understanding of ALS pathogenesis.

METHODS
Participants
Participants with ALS (23; 16 men and 7 women; median age 67 years, range 45–73 years) diagnosed with El Escorial definite, probable or laboratory-supported ALS were recruited from Brighton and Sussex University Hospitals NHS Trust. All had vital capacity (VC) values of over 60% predicted and capacity to give fully informed consent. Exclusion criteria were any contraindication to MRI or inability to tolerate lying flat for 1 hour due to either severe illness or respiratory compromise. Healthy controls (23; 14 men and 9 women, median age 64 years, range 43–76 years) were included in the study for comparison. Genetic screening for known ALS mutations was not carried out for ethical reasons.

Clinical assessments of participants with ALS
Participants with ALS underwent a standardised neurological examination, the Revised ALS Functional Rating Scale (ALSFRS-R)[22] and the Edinburgh Cognitive and Behavioural ALS Screen (ECAS).[23] The clinical assessment was used to stratify participants with ALS according to the site of ALS onset, disease distribution at the time of assessment, disease duration, Medical Research Council (MRC)[24] manual muscle testing power score and upper motor neuron (UMN)[3] score. The ALSFRS-R was used to calculate the monthly rate of change in ALSFRS-R (ΔALSFRS-R; reduction in ALSFRS-R score from 48 at baseline to the score at the time of assessment, divided by the number of months between the two scores), which we used as a substitute for the rate of progression. The ECAS was used to assess for the presence of any cognitive deficits related to the frontotemporal spectrum disorder (ALS-FTSD). These measures were all used to explore for associations between clinical phenotype and NODDI

measures. All except for one of the participants with ALS were taking riluzole at the time of the clinical assessment and MRI.

MRI acquisition
MRI data were acquired on a 1.5T Siemens AVANTO scanner. The acquisition included the following:

1. Dual-echo turbo spin-echo (echo time (TE)=11 and 86 ms; repetition time (TR) =3040 ms; echo-train length=6; field of view (FoV)=240×210 mm^2; matrix=256×224; slice thickness=5 mm).
2. Fast fluid-attenuated inversion recovery (TE=89 ms; TR=9720 ms; inversion time (TI)=2578; echo-train length=16; FoV=240×210 mm^2; matrix=256×224; slice thickness=5 mm).
3. Volumetric high-resolution magnetization prepared rapid gradient echo (MPRAGE) (TE=3.57 ms; TR=2730 ms; TI=100 ms; flip angle=7^0; FoV=256×240 mm^2; matrix=254×240; slice thickness=1 mm).
4. Multishell diffusion-weighted (DW) MRI was acquired with single-shot, twice-refocused pulse-gradient spin-echo (echo planar imaging; EPI),[25] using 3 b-values (9 directions for b=300 smm^{-2}, 30 directions with b=800 smm^{-2} and 60 diffusion directions with b=2400 smm^{-2}), optimised for NODDI.[11 12] Ten non-diffusion-weighted (b=0) volumes were acquired. The following were additional acquisition parameters: TE=99 ms; TR=8400; FoV=240×240 mm^2; matrix=96×96; slice thickness=2.5 mm.

In addition, we also obtained resting-state functional MRI and quantitative magnetisation transfer data (reported elsewhere). The total acquisition time was approximately 1 hour, although the time required for the sequences detailed above was 30 min.

Image processing
The DW images were first corrected for eddy-current distortions and for involuntary movement, using the following pipeline. A 'within-b-value' coregistration was performed, and the average b=0, b=300, b=800 and b=2400 images were created. Each of these averages was coregistered to the mean b=0 image to obtain the transformation matching them. Each DW volume was realigned to the mean DW image with the same b-value, and the final transformation matching each DW volume with the b=0 image was obtained by combining the matrices from either step. The b-matrices were rotated accordingly.[26]

The resulting images were skull-stripped using the FMRIB Software Library (FSL) brain extraction tool (http://fsl.fmrib.ox.ac.uk/fslwiki). Data were analysed using the software distributed by the developers of NODDI (http://www.nitrc.org/projects/noddi_toolbox), implemented in Matlab (V.2012b), which yielded maps of the neurite density index (NDI), orientation dispersion index (ODI) and free water volume fraction for each participant (isotropic compartment (ISO)).[11] Camino (camino.org.uk) was used to fit the diffusion tensor to the same data using weighted least squares regression and to compute FA and MD maps.

The FA images were warped to common space to create a group-specific template, using Advanced Normalization Tools V.2.1.0 (http://stnava.github.io/ANTs). The resulting template was coregistered with the Montreal Neurological Institute (MNI) template from the FSL. The combination of these two transformations was applied to each NODDI parametric map, FA and MD. Three-dimensional Gaussian smoothing with full width at half maximum of 6 mm was performed in SPM12 (http://www.fil.ion.ucl.ac.uk/spm/).

Table 1 Participant demographics and clinical characteristics

Characteristics	Participants with ALS (n=23)	Healthy controls (n=23)
Age, median (range), years	67 (45–73)	64 (43–76)
Sex, n		
Male	16	14
Female	7	9
Site of onset		
Limb	20	–
Bulbar	3	
Disease distribution clinically		
Bulbar and limb involvement	11	–
Limb only involvement	12	
Disease duration, median (range), months	17 (9–39)	–
Slow vital capacity, median (range), %	79 (61–127)	–
UMN score, median (range), out of a maximum of 16 points	8 (3–16)	–
Total MRC power score, median (range), out of a maximum of 220 points	188 (91–220)	–
ALSFRS-R, median (range), out of a maximum of 48 points	40 (25–46)	–
ΔALSFRS-R, median (range)	0.37 (0.09–1.33)	–
ECAS total, median (range), out of a maximum of 136 points	133 (88–135)	–

ALS, amyotrophic lateral sclerosis; ALSFRS-R, Revised ALS Functional Rating Scale; ΔALSFRS-R, rate of change per month in the Revised ALS Functional Rating Scale; ECAS, Edinburgh Cognitive and Behavioural ALS Screen; MRC, Medical Research Council; UMN, upper motor neuron.

Statistical analysis

Statistical Package for the Social Sciences (SPSS IBM V. 22 for Windows) was used for statistical analysis of the demographic data.

Voxel-wise comparisons of whole brain NDI, ODI, ISO, FA and MD maps between the ALS and control groups were performed within the framework of the general linear model of SPM12.

The ALS group was then divided into two subgroups based on the presence or absence of bulbar symptoms (11 bulbar plus limb vs 12 limb alone). Voxel-wise whole brain analysis of NDI, ODI and ISO maps between the ALS subgroups was performed using the general linear model framework within SPM12.

Finally significant associations between the NODDI parametric maps and all of the clinical measures of ALS disease severity were assessed using SPM12.

In all analyses in SPM12, the age of the participant was used as a covariate. The results were accepted as significant where $p < 0.05$ after family-wise error correction at the cluster level, where clusters were formed using $p < 0.001$.

RESULTS

Participant characteristics

The demographics of all participants and the clinical characteristics of participants with ALS are summarised in table 1. The two groups were well matched in terms of age (t=1.11, p=0.27) and gender (χ^2=0.38, p=0.53).

Clinically the ALS group was phenotypically heterogeneous with a wide breadth of weakness, functional disability, rate of progression and cognitive deficit.

The majority of participants with ALS had the typical mixture of upper and lower motor neuron involvement. We recruited four ALS participants with lower motor neuron (LMN)-predominant ALS (two flail arm, two flail leg) and one participant with UMN-predominant phenotype.

None of the participants with ALS fulfilled the revised diagnostic criteria for ALS-Frontotemporal Dementia ALS-FTD.[27]

However five participants with ALS met the criteria for ALS-FTSD: one with ALS cognitive and behavioural impairment and four with ALS cognitive impairment. Six of the participants with ALS had abnormal subscores but did not meet the criteria for ALS cognitive impairment, and one patient had an isolated borderline language subscore.

Neurite orientation dispersion and density imaging

In the whole brain analysis of NODDI parameters, NDI was reduced in the ALS group bilaterally within a large continuous region of the CST extending from the posterior limb of the internal capsule rostrally through the corona radiata into the subcortical WM of the PCG (p<0.001) (figure 1 and table 2). The area of decreased NDI also extended into the transcallosal connection fibres between the primary motor cortices (figure 1A and table 2).

A region within the right anterior internal capsule was detected where ODI was reduced in the ALS group (p=0.014). This contiguous cluster extended into the right PCG (figure 1B and table 2).

Finally, ISO was increased within the region of the right lateral ventricle (p=0.006) (figure 1C and table 2).

Diffusion tensor imaging

In the whole brain analysis of DTI parameters, FA was reduced in the ALS group bilaterally within the two regions of the CST: the pontine CST (p=0.006) and the superior corona radiata and subcortical WM of the PCG (right p<0.001, left p=0.002) (figure 2A and table 2).

MD was significantly increased in the ALS group within the internal capsule of the left CST (p=0.048) (figure 2B and table 2). No changes in MD were detected in the brainstem portion of the CST or the corpus callosum.

Subgroup analysis using the NODDI parameters

Whole brain analysis for differences between subgroups revealed that NDI was significantly reduced in the corona radiata and
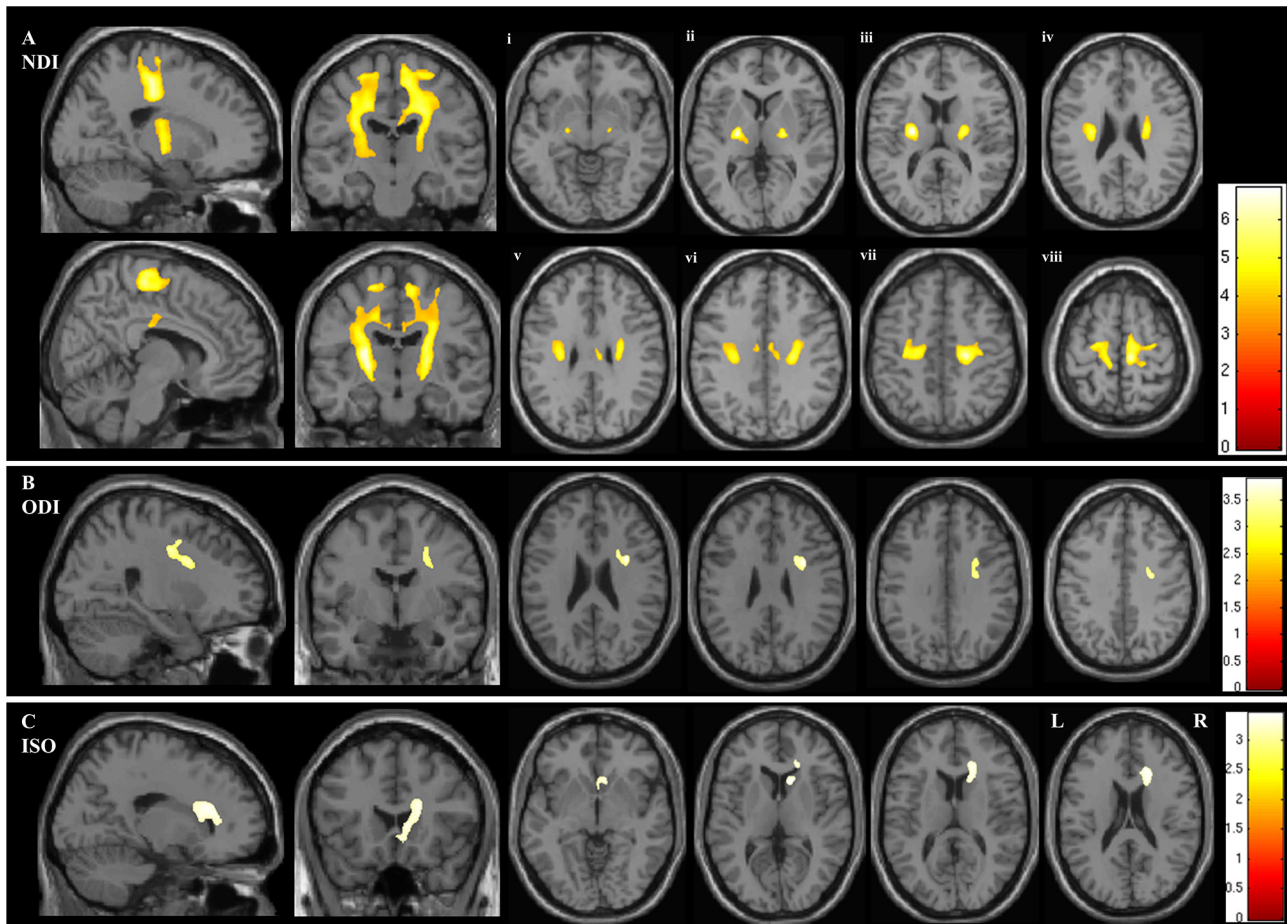
Figure 1 Figure demonstrating the areas of significant difference between the ALS and control groups on whole brain analysis of the NODDI parameters (A) neurite density index (NDI), (B) orientation dispersion index (ODI) and (C) isotropic compartment (ISO). The results are shown using a statistical significance of p<0.05 after family-wise error correction at the cluster level, clusters formed using p<0.001. Figures Ai - Aviii demonstrate the the areas of significant difference in NDI on axial sections from the posterior limb of the internal capsule (vi) extending rostrally up into the subcortical WM of the PCG (viii).

subcortical WM of the right hemisphere in the subgroup with both bulbar and limb involvement, compared with those with limb-only involvement (figure 3).

There were no significant differences in ODI or ISO between these ALS subgroups.

Correlation of NODDI parameters with disease severity

Using whole brain analysis of NODDI parameters, both ODI and ISO showed significant correlation with disease duration. ODI correlated with disease duration predominantly in the right PCG, but also with a smaller region in the medial aspect of the left PCG (see figure 4A). Further areas where ODI correlated significantly with disease duration were detected within the precuneus and the dorsolateral prefrontal cortex bilaterally. The ISO correlated with disease duration in the interhemispheric fissure, in close proximity to the paracentral lobule and precuneus, as well as the fourth ventricle (see figure 4B).

No significant correlations were found between the NODDI parameters and measures of disease severity: ALSFRS-R, ΔALSFRS-R, UMN score, MRC power score and ECAS.

DISCUSSION

The major findings in this study using NODDI in ALS relate, firstly, to significant reduction of NDI in the CST and corpus callosum in ALS, suggesting loss of axonal density in these pathways. Secondly,

the reduction of ODI within the PCG in the ALS group and the correlation of ODI with disease duration suggest a relationship between cortical pathology and the severity of the ALS disease process. Finally, our results are consistent with previous DTI findings; however, NODDI provides a more definitive interpretation of the microstructural changes underlying ALS by separating neurite density from orientation dispersion.

In relation to the WM changes, the area of reduced NDI extends from the posterior limb of the internal capsule and continues rostrally into the subcortical WM of the PCG. This supports the notion that loss of motor neuron axon density within the cerebral WM is a core feature of the neurodegenerative process associated with ALS, consistent with many pathological studies.[28 29] It is possible that alterations in glial cells and myelin may also contribute to these changes in NDI. However, as the density of axons per voxel is much higher than that of glial cells, and loss of motor neuron axons is a key feature of ALS, we expect that the largest changes are explained by axonal loss.

Regarding reductions in the NDI and ODI in the PCG, we interpret these changes as compatible with the loss of dendritic density and reduced dendritic arborisation within the motor cortex, as suggested by recent histopathological analyses in humans and animal models.[30 31] Although changes in cortical dendrites are observed at early stages of disease evolution in animal models of ALS,[32 33] the cortical findings in our cohort using NODDI are

Table 2 Regions of significant differences in quantitative diffusion imaging parameters between ALS and control (CTL) groups

Contiguous anatomical regions within cluster	MNI coordinate (x, y, z)	t-Value	K (size)	P$_{clusterlevelFWE-corr}$
NDI (ALS<CTL)				
Right cerebral cortex, precentral gyrus	11, −25, 60	5.85	15 344	<0.001
Right cerebral WM, corticospinal tract	22, −22, 46	5.69		
Right posterior limb of the internal capsule	23, −12, 7	5.21		
Left posterior limb of the internal capsule	−24, −11, 12	6.23	14 005	<0.001
Left cerebral WM, corticospinal tract	−13, −28, 58	5.32		
Left superior corona radiata	−20, −20, 41	4.91		
ODI (ALS<CTL)				
Right precentral gyrus	32, 5, 27	3.89	1847	0.014
Right precentral gyrus	25, −1, 44	3.60		
Right anterior internal capsule	21, 9, 21	3.59		
ISO (ALS>CTL)				
Right caudate, lateral ventricle	11, 18, 4	3.45	2960	0.006
Right anterior corona radiata	20, 23, 19	3.39		
Right genu of corpus callosum	8, 25, 8	3.30		
FA (ALS<CTL)				
Right precentral gyrus	15, −23, 66	5.10	4097	<0.001
Right cerebral corticospinal tract	26, −23, 49	4.36		
Right superior corona radiata	18, −21, 42	4.19		
Left cerebral WM, corticospinal tract	−15, −23, 67	5.25	2877	0.002
Left cerebral cortex, precentral gyrus	−21, −18, 70 −18, −15, 59	4.32 4.08		
Right pons, corticospinal tract	7, −26, −37	5.11	2309	0.006
Right brainstem, corticospinal tract	3, −34, −47	5.10		
Left pons, corticospinal tract	−7, −23, −36	4.69		
MD (ALS>CTL)				
Left superior corona radiata	−24, −19, 35	4.78	3315	0.048
Left posterior limb of the internal capsule	−18, −15, 3 −20, −17, 14	3.55 3.43		

The table shows the anatomical regions where significant changes were demonstrated on whole brain analysis in neurite density index (NDI), orientation dispersion index (ODI), isotropic compartment (ISO), fractional anisotropy (FA), and mean diffusivity (MD). A statistical significance threshold of p<0.05 family-wise error (FWE) correction at the cluster level (P$_{cluster}$) was used, after clusters were formed with an uncorrected p<0.001. Montreal Neurological Institute (MNI) coordinates were used to define the anatomical location of each cluster of voxels within the MRI volume. The MNI coordinates refer to the peak t-value. Local maxima that are more than 8 mm apart are shown for each cluster. K indicates the size of the cluster in voxels.
ALS, amyotrophic lateral sclerosis; WM, white matter.

limited to a region within the right PCG. It is possible that pathological heterogeneity within the primary motor cortex contributes to difficulties in detecting consistent alterations in cortical areas using current imaging techniques for whole brain comparisons or that loss of cortical dendrites is a relatively late phenomenon in the evolution of cerebral pathology in ALS. Nonetheless, these findings indicate that NODDI can reveal new aspects of the cellular pathology of diseases such as ALS, in keeping with the recent demonstration that changes in NODDI parameters closely reflect complex histological changes in the grey matter (GM) and in the WM of the spinal cord in multiple sclerosis.[13]

A direct comparison of the NDI and FA whole brain findings in our study shows that NDI detected larger areas of neurodegeneration than FA at the same statistical threshold, where the combined cluster sizes for the areas of significantly reduced NDI (29 349) were greater than those for areas of significantly reduced FA (9283) (see table 2). This suggests that NDI may have a higher sensitivity than FA for detecting ALS-related WM pathology and also indicates that the primary pathology identified by the diffusion MRI signal is alteration in axon density.

In our study FA was reduced into two separate regions of the CST in the ALS group, one within the pons and another within the corona radiata extending into the subcortical WM of the PCG. The CST has previously been implicated in DTI studies demonstrating reduced FA in the ALS group.[34–36] Typically studies report reduced FA in one or several isolated regions, including the pons, cerebral peduncles, posterior limb of the internal capsule, corona radiata and the subcortical WM of the PCG.[3 4 35 36] Low FA within the corpus callosum is also typically demonstrated in ALS[37] but not always.[4] Rarely are such extensive, contiguous changes demonstrated throughout the CST and corpus callosum, as evident with our findings of reduced NDI using NODDI.
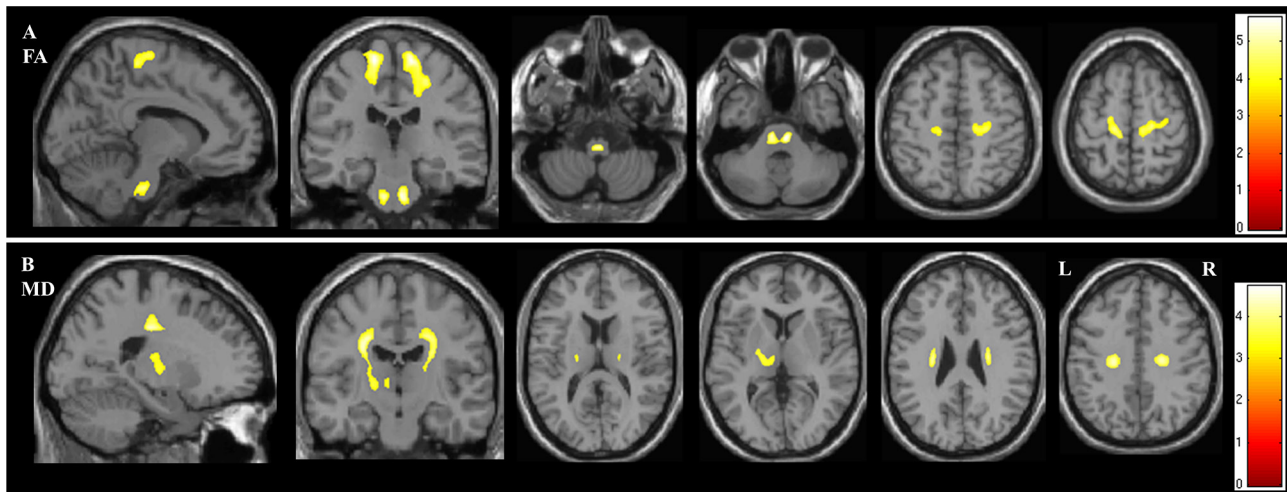
Figure 2 Figure demonstrating the areas of significant difference between the ALS and control groups on whole brain analysis of DTI parameters (A) fractional anisotropy (FA) and (B) mean diffusivity (MD). The results are shown using a statistical significance of p<0.05 after family-wise error correction at the cluster level, clusters formed using p<0.001.

We found increased MD in the ALS group within the left internal capsule, which is consistent with previous studies.[3] Reports of increased MD have been less consistent than FA findings in ALS, which may be explained by the known dependency of MD on the specific b-value used for the acquisition.[26] In this study, we used a maximum b-value of 2400 smm^{-2}, which is higher than typical DTI protocols and may account for our findings. We could have restricted our DTI analysis to the inner shell (b=800) data to make it more compatible with other DTI studies. However this would have made the comparison with NODDI (fitted with the full data set) unfair. In general the extent of WM changes we found using DTI is somewhat reduced compared with other studies.[3 4 34–37] This might be the consequence of specific methodological differences, the relatively small sample size or the clinical heterogeneity of the cohort.

NODDI facilitates the interpretation of the altered diffusivity profile in ALS observed using DTI where axonal loss, demonstrated by reduced NDI in the CST and corpus callosum, is likely to be the main contributing factor for the reduced FA and increased MD. We detected reduced ODI in the right internal capsule, a region where there is crossing of WM pathways. This could be explained by the predominant degeneration of axonal fibres in one direction, thereby reducing crossing of fibres in this region. Furthermore, this may contribute to the lack of changes in FA detected in this region as the corresponding FA may not change due to the remaining fibres becoming more coherent, despite axonal degeneration.

Increased ISO was detected within the right lateral ventricle, likely representing atrophy in ALS, leading to increased CSF spaces.

When subgroup analysis was performed, the ALS subgroup with both bulbar and limb involvement showed loss of right CST axon density significantly greater than the group with limb-confined ALS. This is in keeping with our hypothesis that more widespread clinical involvement in ALS relates to more extensive microstructural damage.

Regression analysis revealed that both ODI and ISO correlated with disease duration, where regions of the right PCG and interhemispheric fissure were involved, respectively. This suggests that loss of cortical dendrites and related cerebral atrophy are occurring alongside axonal degeneration. The correlation of ODI in the PCG with disease duration provides support for the rationale that loss of complex neuropil architecture within the motor cortex is occurring in ALS over time.

Clinical heterogeneity of the ALS participants in this study was considerable, which could explain why we failed to detect a significant group difference in more regions of the PCG. A larger study using a more homogeneous ALS phenotype may be required in order to achieve this on whole brain analysis of ODI. Although statistically significant cortical GM changes in ODI and NDI were limited to a region within the right PCG, these abnormalities could be more relevant to the site and severity of disease. Moreover, the topographical pattern of disease within the PCG in ALS is likely to have a larger spread of regions involved, with higher variability
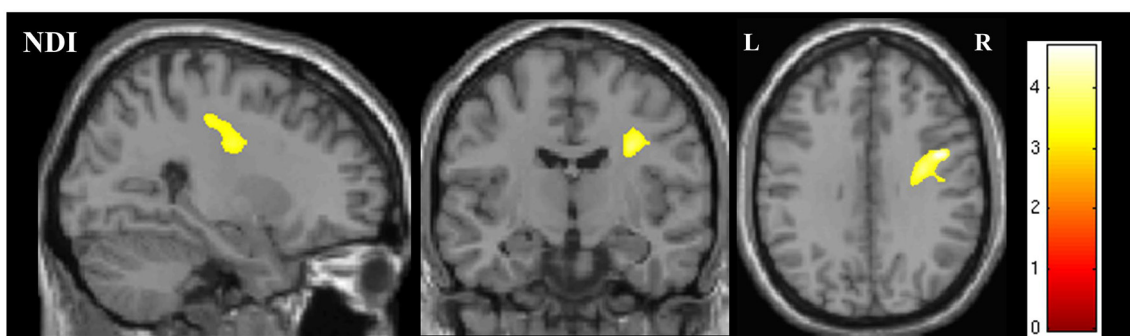

Figure 3 Figure showing the region of significant difference in NDI on whole brain analysis between the bulbar plus limb ALS group and the limb-confined ALS group. The results are shown for p<0.05 after family-wise error correction at the cluster level, clusters formed using p<0.001.
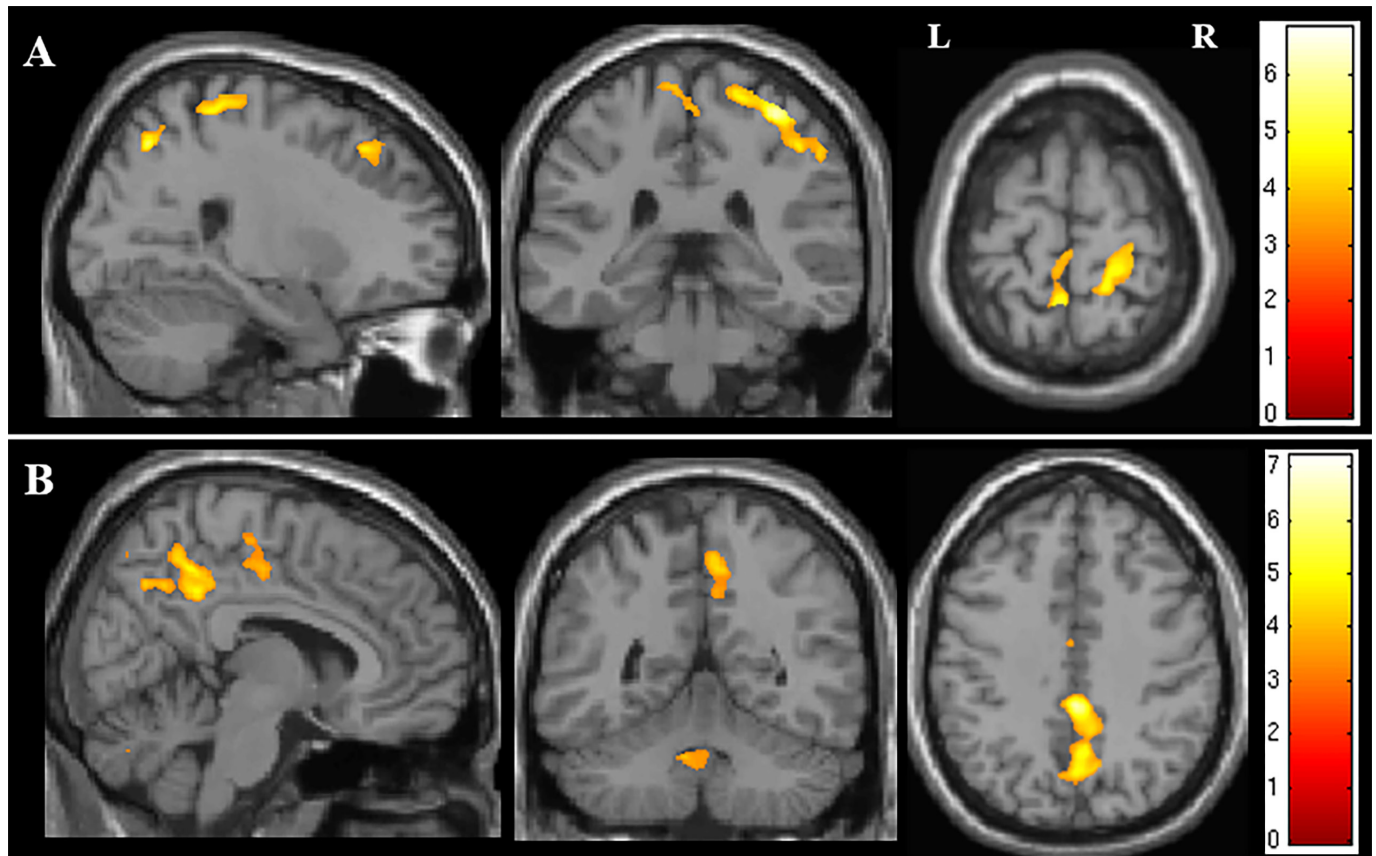
Figure 4 Figure showing the areas of correlation on whole brain analysis of NODDI parameters and measures of disease severity. (A) Areas of correlation between orientation dispersion index and disease duration. (B) Areas of correlation between isotropic compartment and disease duration. The results are shown for p<0.05 after family-wise error correction at the cluster level, clusters formed using p<0.001.

between patients, when compared with the converging axons of the CST, the common output pathway of all cortical motor fibres. This reduces the detection of significant differences on whole brain analysis, which may therefore only become more apparent in larger cohorts. Although the GM results are not as strong as those obtained in the WM, they nevertheless support the hypothesis of dendritic abnormalities paralleling disease progression.

We recognise that there are limitations related to the technique used in this study. NODDI may not separate the effects of orientation dispersion and neurite density effectively within the GM and may therefore not fully distinguish intracortical neuropil pathology in ALS.[38] More recently developed quantitative diffusion MRI techniques, incorporating microscopic anisotropy mapping, may separate different signal components better and highlight differences more effectively[39 40] but would require additional imaging sequences that are not yet available clinically. The NODDI technique used in this study[11] models orientation dispersion isotropically and may therefore be limited in its capacity to model multiple fibre orientations arising from complex dendritic structures.[7] NODDI has subsequently been developed further to incorporate a quantification of anisotropic orientation dispersion, and analysis using this more sophisticated modelling system is warranted in future studies in ALS.[12]

We used whole brain voxel-wise analysis, which does not require any a priori hypotheses and provides information about changes in both WM and GM. Although whole brain analysis is prone to potential biases due to interindividual anatomical variation and partial volume effects, NODDI has the advantage over DTI of explicitly modelling the free water (isotropic) component and

should therefore be less susceptible to the partial volume contamination of CSF. Alternative processing approaches to whole brain analysis, such as tract-based spatial statistics[41] and GM special statistics,[14] have been optimised to minimise the potential sources of error and to detect changes in WM and GM, respectively. Tractometry, which maps quantitative indices (such as those derived from NODDI) to points of streamlines reconstructed by diffusion tractography, is a powerful visualisation tool and can potentially give insight into the regions of degeneration but suffers from well-known limitations.[42]

It should also be noted that many of the studies using NODDI[14 15] were performed at 3T, while our data were performed at 1.5T. The field strength has obvious implication for the signal to noise ratio (SNR). However, the reduced signal intensity at 1.5T is partially compensated by the longer T2 relaxation time at this field strength. We used a voxel size of 2.5 mm^3, which is almost twice as large as that used in the original NODDI paper[11] at 3T, and should ensure a comparable SNR at the price of reduced spatial resolution.

Another limitation is the sample size, which is particularly relevant given emerging insights into disease heterogeneity in ALS.[1] Nevertheless, our findings illustrate the potential for NODDI to interrogate hitherto undetectable details of cellular pathology of ALS in life.

We conclude that NODDI reveals evidence compatible with structural damage in the PCG in ALS, provides new insights into the cellular pathology of WM damage, and demonstrates that reduced density of corticospinal axons is the main contributing factor underlying the altered diffusivity profile detected by DTI. Our observations are compatible with relatively early involvement

of cortical neuropil including dendrites in ALS. More extensive longitudinal studies in larger phenotypically and genetically defined cohorts will be needed to refine further studies on the cortical microstructure in ALS using NODDI and developments thereof.

REFERENCES

1 van Es MA, Hardiman O, Chio A, et al. Amyotrophic lateral sclerosis. *Lancet* 2017;390:2084–98.
2 Cavanagh JB. The problems of neurons with long axons. *Lancet* 1984;1:1284–7.
3 Ellis CM, Simmons A, Jones DK, et al. Diffusion tensor MRI assesses corticospinal tract damage in ALS. *Neurology* 1999;53:1051–8.
4 Canu E, Agosta F, Riva N, et al. The topography of brain microstructural damage in amyotrophic lateral sclerosis assessed using diffusion tensor MR imaging. *AJNR Am J Neuroradiol* 2011;32:1307–14.
5 Jelescu IO, Veraart J, Fieremans E, et al. Degeneracy in model parameter estimation for multi-compartmental diffusion in neuronal tissue. *NMR Biomed* 2016;29:33–47.
6 Vos SB, Jones DK, Jeurissen B, et al. The influence of complex white matter architecture on the mean diffusivity in diffusion tensor MRI of the human brain. *Neuroimage* 2012;59:2208–16.
7 Jeurissen B, Leemans A, Tournier JD, et al. Investigating the prevalence of complex fiber configurations in white matter tissue with diffusion magnetic resonance imaging. *Hum Brain Mapp* 2013;34:2747–66.
8 Ennis DB, Kindlmann G. Orthogonal tensor invariants and the analysis of diffusion tensor magnetic resonance images. *Magn Reson Med* 2006;55:136–46.
9 Jespersen SN, Kroenke CD, Østergaard L, et al. Modeling dendrite density from magnetic resonance diffusion measurements. *Neuroimage* 2007;34:1473–86.
10 Jespersen SN, Leigland LA, Cornea A, et al. Determination of axonal and dendritic orientation distributions within the developing cerebral cortex by diffusion tensor imaging. *IEEE Trans Med Imaging* 2012;31:16–32.
11 Zhang H, Schneider T, Wheeler-Kingshott CA, et al. NODDI: practical in vivo neurite orientation dispersion and density imaging of the human brain. *Neuroimage* 2012;61:1000–16.
12 Tariq M, Schneider T, Alexander DC, et al. Bingham-NODDI: mapping anisotropic orientation dispersion of neurites using diffusion MRI. *Neuroimage* 2016;133:207–23.
13 Grussu F, Schneider T, Tur C, et al. Neurite dispersion: a new marker of multiple sclerosis spinal cord pathology? *Ann Clin Transl Neurol* 2017;4:663–79.
14 Nazeri A, Chakravarty MM, Rotenberg DJ, et al. Functional consequences of neurite orientation dispersion and density in humans across the adult lifespan. *J Neurosci* 2015;35:1753–62.
15 Kamagata K, Hatano T, Okuzumi A, et al. Neurite orientation dispersion and density imaging in the substantia nigra in idiopathic Parkinson disease. *Eur Radiol* 2016;26:2567–77.
16 Colgan N, Siow B, O'Callaghan JM, et al. Application of neurite orientation dispersion and density imaging (NODDI) to a tau pathology model of Alzheimer's disease. *Neuroimage* 2016;125:739–44.
17 Adluru G, Gur Y, Anderson JS, et al. Assessment of white matter microstructure in stroke patients using NODDI. *Conf Proc IEEE Eng Med Biol Soc* 2014;2014:742–5.
18 Winston GP, Micallef C, Symms MR, et al. Advanced diffusion imaging sequences could aid assessing patients with focal cortical dysplasia and epilepsy. *Epilepsy Res* 2014;108:336–9.
19 Rae CL, Davies G, Garfinkel SN, et al. Deficits in neurite density underlie white matter structure abnormalities in first-episode psychosis. *Biol Psychiatry* 2017;82:716–25.
20 Fogarty MJ, Noakes PG, Bellingham MC. Motor cortex layer V pyramidal neurons exhibit dendritic regression, spine loss, and increased synaptic excitation in the presymptomatic hSOD1(G93A) mouse model of amyotrophic lateral sclerosis. *J Neurosci* 2015;35:643–7.
21 Herms J, Dorostkar MM. Dendritic spine pathology in neurodegenerative diseases. *Annu Rev Pathol* 2016;11:221–50.
22 Cedarbaum JM, Stambler N, Malta E, et al. The ALSFRS-R: a revised ALS functional rating scale that incorporates assessments of respiratory function. BDNF ALS Study Group (Phase III). *J Neurol Sci* 1999;169:13–21.
23 Abrahams S, Newton J, Niven E, et al. Screening for cognition and behaviour changes in ALS. *Amyotroph Lateral Scler Frontotemporal Degener* 2014;15:9–14.
24 Medical Research Council. *Aids to the investigation of the peripheral nerve injuries. her majesty's stationary office*, 1976.
25 Reese TG, Heid O, Weisskoff RM, et al. Reduction of eddy-current-induced distortion in diffusion MRI using a twice-refocused spin echo. *Magn Reson Med* 2003;49:177–82.
26 Leemans A, Jones DK. The B-matrix must be rotated when correcting for subject motion in DTI data. *Magn Reson Med* 2009;61:1336–49.
27 Strong MJ, Abrahams S, Goldstein LH, et al. Amyotrophic lateral sclerosis - frontotemporal spectrum disorder (ALS-FTSD): revised diagnostic criteria. *Amyotroph Lateral Scler Frontotemporal Degener* 2017;18:153–74.
28 Brownell B, Oppenheimer DR, Hughes JT. The central nervous system in motor neurone disease. *J Neurol Neurosurg Psychiatry* 1970;33:338–57.
29 Smith MC. Nerve fibre degeneration in the brain in amyotrophic lateral sclerosis. *J Neurol Neurosurg Psychiatry* 1960;23:269–82.
30 Genç B, Jara JH, Lagrimas AK, et al. Apical dendrite degeneration, a novel cellular pathology for Betz cells in ALS. *Sci Rep* 2017;7:41765.
31 Fogarty MJ, Mu EW, Noakes PG, et al. Marked changes in dendritic structure and spine density precede significant neuronal death in vulnerable cortical pyramidal neuron populations in the SOD1(G93A) mouse model of amyotrophic lateral sclerosis. *Acta Neuropathol Commun* 2016;4:77.
32 Fogarty MJ, Klenowski PM, Lee JD, et al. Cortical synaptic and dendritic spine abnormalities in a presymptomatic TDP-43 model of amyotrophic lateral sclerosis. *Sci Rep* 2016;6:37968.
33 Jara JH, Villa SR, Khan NA, et al. AAV2 mediated retrograde transduction of corticospinal motor neurons reveals initial and selective apical dendrite degeneration in ALS. *Neurobiol Dis* 2012;47:174–83.
34 Iwata NK, Kwan JY, Danielian LE, et al. White matter alterations differ in primary lateral sclerosis and amyotrophic lateral sclerosis. *Brain* 2011;134(Pt 9):2642–55.
35 Agosta F, Valsasina P, Riva N, et al. The cortical signature of amyotrophic lateral sclerosis. *PLoS One* 2012;7:e42816.
36 Zhang Y, Schuff N, Woolley SC, et al. Progression of white matter degeneration in amyotrophic lateral sclerosis: A diffusion tensor imaging study. *Amyotroph Lateral Scler* 2011;12:421–9.
37 Filippini N, Douaud G, Mackay CE, et al. Corpus callosum involvement is a consistent feature of amyotrophic lateral sclerosis. *Neurology* 2010;75:1645–52.
38 Lampinen B, Szczepankiewicz F, Mårtensson J, et al. Neurite density imaging versus imaging of microscopic anisotropy in diffusion MRI: a model comparison using spherical tensor encoding. *Neuroimage* 2017;147:517–31.
39 Shemesh N, Cohen Y. Microscopic and compartment shape anisotropies in gray and white matter revealed by angular bipolar double-PFG MR. *Magn Reson Med* 2011;65:1216–27.
40 Szczepankiewicz F, Lasič S, van Westen D, et al. Quantification of microscopic diffusion anisotropy disentangles effects of orientation dispersion from microstructure: applications in healthy volunteers and in brain tumors. *Neuroimage* 2015;104:241–52.
41 Smith SM, Jenkinson M, Johansen-Berg H, et al. Tract-based spatial statistics: voxelwise analysis of multi-subject diffusion data. *Neuroimage* 2006;31:1487–505.
42 Campbell JS, Pike GB. Potential and limitations of diffusion MRI tractography for the study of language. *Brain Lang* 2014;131:65–73.